Article

Sphingomyelin synthase 1 supports two steps of rubella virus life cycle

Mayuko Yagi,
Minami Hama,
Sayaka Ichii, ...,
Takako Kurata,
Kosuke Yusa, Jun
Komano

jun.komano@ompu.ac.jp

Highlights

SGMS1 was identified as a positive regulator of rubella virus replication

Rubella virus did not infect cells lacking the expression of SGMS1

SGMS1 had two action points during the life cycle of rubella virus

Article

Sphingomyelin synthase 1 supports two steps of rubella virus life cycle

Mayuko Yagi,[1] Minami Hama,[1] Sayaka Ichii,[1] Yurie Nakashima,[1] Daiki Kanbayashi,[2] Takako Kurata,[2] Kosuke Yusa,[3] and Jun Komano[1,4,*]

SUMMARY

Our knowledge of the regulatory mechanisms that govern the replication of the rubella virus (RV) in human cells is limited. To gain insight into the host-pathogen interaction, we conducted a loss-of-function screening using the CRISPR-Cas9 system in the human placenta-derived JAR cells. We identified *sphingomyelin synthase 1* (*SGMS1* or *SMS1*) as a susceptibility factor for RV infection. Genetic knockout of *SGMS1* rendered JAR cells resistant to infection by RV. The re-introduction of *SGMS1* restored cellular susceptibility to RV infection. The restricted step of RV infection was post-endocytosis processes associated with the endosomal acidification. In the late phase of the RV replication cycle, the maintenance of viral persistence was disrupted, partly due to the attenuated viral gene expression. Our results shed light on the unique regulation of RV replication by a host factor during the early and late phases of viral life cycle.

INTRODUCTION

Rubella is a contagious viral disease mostly affecting children.[1] It is generally a self-limiting disease characterized by fever, catarrh, and rash. It has been successfully controlled in many geographic areas, mainly via the administration of a live-attenuated vaccine. Rubella virus (RV) infects the placental tissue upon viremia, and is transmitted to the fetus via the transplacental route. RV infection can lead to congenital disorders in infants or even fetal death.[2] The former is known as congenital rubella syndrome (CRS), which occurs most frequently when the mother is infected with RV during the first trimester, the early stage of pregnancy. The type of birth defects depends on the gestational age at the time of RV infection. The lack of understanding of the molecular interaction between the virus and its host is partly due to rubella being a vaccine-preventable disease. The molecular basis of RV teratogenicity remains largely unclear.

RV belongs to the genus *Rubivirus* of the family *Matonaviridae*. It has a single-stranded positive-sense RNA as a genome. RV replicates in many tissue culture cell lines and establishes persistent infection, including African green monkey-derived Vero, rabbit kidney-derived RK13, and baby hamster kidney-derived BHK. Not many human-derived cell lines can support the persistent RV infection[3–5]; however, persistent infection is found in RV-infected individuals.[6] Basic research on RV replication has been conducted in human-derived primary and established cells as well as non-human mammalian cell lines; nevertheless, the natural host of RV is solely the humans. Although the receptor of RV has not yet been determined, a candidate molecule has been reported.[7] Once RV is attached to the cells, it enters them via clathrin-dependent endocytosis.[8] Virus-cell membrane fusion depends on the acidic environment and calcium ions in the endosome.[9] RV replication occurs in a membrane-surrounded microstructure, named replication complex (RC) or cytopathic vacuole, the formation of which involves cellular organelles, including the endoplasmic reticulum, lysosome, mitochondria, and Golgi apparatus.[10,11] Replication foci should be passed onto daughter cells to maintain the viral persistence although the precise mechanisms remained unclear. Only a limited number of host cell factors are identified to help support the viral replication.[12–14]

Recent advances in genome-editing technology, based on the CRISPR-Cas9, have enabled loss-of-function screening at the genetic level. CRISPR-Cas9 can irreversibly dysregulate targeted genes. A systematic genetic knockout strategy adopting the CRISPR-Cas9 system complements cDNA-based gain-of-function screens as well as loss-of-function screens adopting RNA interference that partially limits target gene expression. Loss-of-function screen is applicable for identifying genes susceptible to cell-damaging agents, such as toxins. RV infection results in apoptotic cell death in many cell lines.[15,16] Thus, CRISPR-Cas9-based genetic loss-of-function screening would be suitable for exploring positive regulatory factors that allow the RV infection.

This study aimed to conduct a genome-wide loss-of-function screening to identify the genes necessary for the RV infection in human cells. Among the eight candidate genes identified, we investigated *sphingomyelin* (SGM) *synthase 1* (*SGMS1* or *SMS1*) whether it serves as a positive regulator of RV infection.

[1]Department of Microbiology and Infection Control, Faculty of Pharmacy, Osaka Medical and Pharmaceutical University, 4-20-1 Nasahara, Takatsuki City, Osaka 569-1041, Japan
[2]Osaka Institute of Public Health, Morinomiya Center, 1-3-69, Nakamichi, Higashinari-ku, Osaka 537-0025, Japan
[3]Stem Cell Genetics, Institute for Frontier Life and Medical Sciences, Kyoto University, Kyoto 606-8507, Japan
[4]Lead contact
*Correspondence: jun.komano@ompu.ac.jp
https://doi.org/10.1016/j.isci.2023.108267
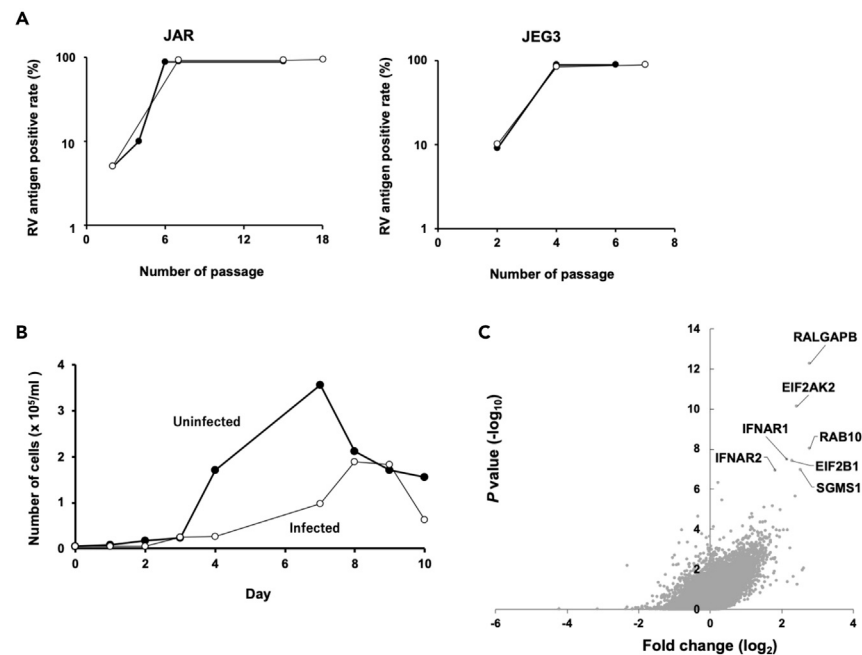
Figure 1. CRISPR-Cas9-based knockout screening to identify host regulatory factors for RV replication

(A) Establishment of RV persistency in JAR and JEG3 cells after several passages. The percentage of viral antigen-positive cells was evaluated by IFA. Filled, field isolate; open, vaccine strain.

(B) Cell growth kinetics of RV_{VAC}-infected JAR cells. Filled, uninfected; open, infected.

(C) Volcano plots showing the LV-encoded target genes that enriched in the RV_{FI}-infected JAR cells. Each dot represents a gene, and the eight genes with the highest enrichment were noted.

RESULTS

Genetic screening in search of RV infection regulators

In JAR and JEG3 human choriocarcinoma cell lines, RV infection resulted in persistent infection, with almost all the cells testing positive for RV antigens using immunofluorescence assay (IFA) after several passages post-infection, using either vaccine strain Matsuura or a field isolate Osaka2019 (RV_{VAC} and RV_{FI} hereafter, respectively; Figure 1A). Tissue culture supernatant from the persistently infected cells contained infectious virions. The cell growth kinetics of virus-infected cells was slower than that of the parental cells, suggesting that the persistent RV infection had a negative impact on cell growth (Figure 1B).

To identify the positive regulatory factors of RV infection in the host cell, we conducted a loss-of-function screening using JAR cells. We established a JAR cell clone stably expressing SpCas9 and infected it with a lentiviral vector (LV) encoding a gRNA library covering all the human genes in order to produce a cell pool. These cells were further infected with RV_{FI}. Two weeks post infection, we analyzed enriched LV-encoded gRNA repertoire in the RV-infected cells and compared it to that in the RV-uninfected cells (Data S1). We identified eight genes significantly enriched in the RV-infected cells, namely *IFNAR1, EIF2AK2, EIF2B1, RAB10, RALGAPB, SGMS1, IFNAR2,* and *RABIF*, listed on the order of the magnitude of enrichment (Figure 1C).

Four genes were related to interferon (IFN) responses, including receptors of type I interferon (*IFNAR1* and *R2*), an IFN effector (*EIF2AK2* or *PKR*), and a target of the IFN effector (*EIF2B1*). Three genes were involved in the membrane trafficking/vesicular transport, possibly supporting the IFN and/or IFN receptor trafficking (*RAB10, RABIF,* and *RALGAPB*). Since IFN retards the rate of cell proliferation, the selection of these genes in the screen seemed reasonable. *SGMS1* was the only gene that was unrelated to IFN responses according to the literature. SGMS1 is enriched at one week post infection, and the same result was observed when the screening was performed using RV_{VAC}. We focused on *SGMS1* and investigated whether the susceptibility to RV infection could indeed be attenuated by gene disruption.

SGMS1 as a positive regulatory factor in RV infection

JAR cells were transfected with a plasmid that co-expressed SpCas9 and gRNAs that targeted two genomic loci of *SGMS1*. This was done to disrupt the gene by removing a part of it as shown in Figure 2A (Figure 2A). Cells were then selected in the presence of puromycin. Among the 12 clones that were screened, PCR analysis identified two clones, namely #1 and #4, as $SGMS1^{-/-}$, with an isolation frequency of 17% (Figure 2B). Western blot analysis of the representative knockout clone #4 revealed undetectable expression of *SGMS1* protein (Figure 2C). In *SGMS1*-null cell clones, the content of SGM was found to be reduced to 22.2% and 52.3% compared to the control JAR cell clones (Figure 2D), consistent with earlier reports (20%–50%).[17,18] It was observed that SGM could still be supplied to *SGMS1*-null cell clones either through
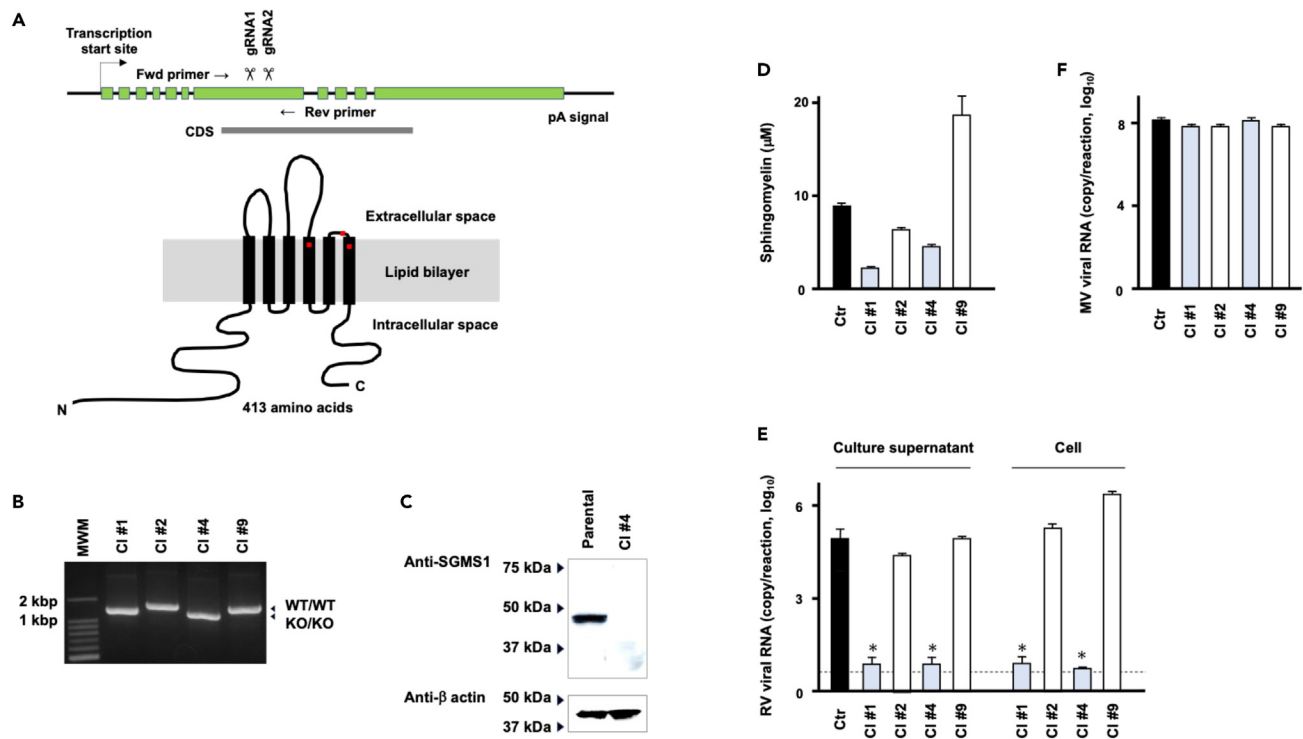
Figure 2. SGMS1 as a positive regulator of RV infection

(A) Schematic diagram of the gene organization and protein structure of *SGMS1*. *SGMS1* contains 11 exons (boxes). The gRNA-targeted genomic loci (scissors) and PCR primers to screen for the gene-disrupted cell clones (arrows) are shown. The red dots represent three key amino and residues, namely H285, H328, and D332, constituting the catalytic center of the SGM synthase activity. CDS, coding sequence; pA, polyadenylation.

(B) Amplification of the *SGMS1* genomic locus of JAR cell clones by PCR. Wild-type (WT) *SGMS1* gene and the knockout (KO) yielded approximately 1.4 and 1.2 kbp products, respectively. MWM, molecular weight markers.

(C) Immunoblotting for *SGMS1* detection in JAR clone #4.

(D) Sphingomyelin content in JAR cell clones. Concentrations corresponding to 1×10^6 cells lysed in 50 μL assay buffer are shown.

(E) Susceptibility of JAR cell clones to RV_{VAC} infection. RNA was harvested from the tissue culture medium and from cells at 9 and 10 days post infection, respectively, and subjected to real-time quantitative RT-PCR. The dashed line indicates the limit of detection (5 copies/reaction).

(F) Susceptibility of JAR cell clones to MeV vaccine strain. Cellular RNA was recovered at 4 days post infection. Clones with $SGMS1^{+/+}$ and $SGMS1^{-/-}$ genotypes are shown in white and blue gray, respectively. Cell clones transduced with both mCherry and puromycin resistance genes were used as controls (Ctr, filled). Data shown in bar graphs represent the average value and the standard deviation (SD) of triplicate reactions. Asterisk, $p < 0.001$ compared to either Ctr, Cl #2, or #4.

endogenous expression of SGMS2 or from the serum-supplemented tissue culture medium. Furthermore, unlike in HeLa cells, rates of cell proliferation were found to be indistinguishable across the cell clones.[19] As per quantitative RT-PCR and IFA analysis, *SGMS1* knockout clones #1 and #4 showed significantly reduced support for replication of both RV_{FI} and RV_{VAC}, while viral genomic RNA was detected at the levels slightly above the detection limit in RNA recovered from either the culture supernatant or cells (Figures 2E and 3B). On the other hand, RV infection in cell clones #2 and #9, bearing $SGMS1^{+/+}$, was comparable to that in the control cells (Figure 2E). To determine the specificity of the loss of susceptibility to RV infection, these cell clones were also exposed to Measles virus (MeV), and the efficiency of infection was then assessed by quantitative RT-PCR. It was observed that all the cell clones supported MeV infection at comparable levels (Figure 2F). Similar observations were made with adenovirus type 5 and vesicular stomatitis virus (VSV)-G-pseudotyped murine leukemia virus (MLV, described later). The data suggested that the genetic loss of *SGMS1* specifically affected RV infection, and did not affect transcription and translation.

SGMS1 encodes a protein with six membrane-spanning domains (Figure 2A). Upon transient transfection of SGMS1 fused to mApple, a red fluorescent protein, at its carboxy terminus, into cell clones #1 and #4, SGMS1-mApple was observed in a punctate pattern in the cytoplasm, mostly around the nucleus and evenly on the plasma membrane (Figure 3A). This distribution pattern was consistent with the previous findings[19] and was also observed in other human cell lines, including HeLa, NP-2, and 293FT cells. The susceptibility of $SGMS1^{-/-}$ clones #1 and #4 to RV infection was restored upon transient or stable expression of SGMS1-mApple, as confirmed by IFA (Figures 3B and 3C). Moreover, ectopic expression of SGMS1-mApple in parental JAR cells resulted in a 2-fold increase in susceptibility to RV replication, as determined by quantitative RT-PCR (Figure 3D). These findings were supported by the observation that the SGM content was approximately 2-fold higher than SGMS1-mApple-expressing cells compared to control cells (Figure 3E). Overall, these results confirm that *SGMS1* is indeed a positive regulatory factor in RV infection.
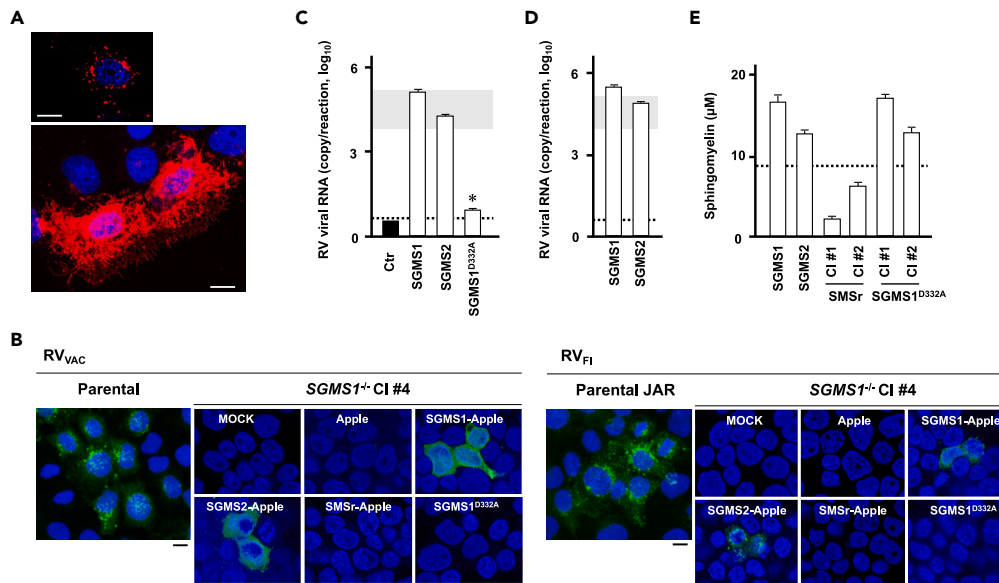
Figure 3. RV infection in cells expressing sphingomyelin synthase gene family

(A) Intracellular distribution of SGMS1-mApple in JAR *SGMS1* null clone #4 imaged by the confocal microscopy with different sensitivities. Red represents the fluorescence of SGMS1-mApple and blue represents DAPI-stained nucleus, respectively. Left, magnification 400×; right, magnification 200×. Scale bar, 10 μm.

(B) Detection of RV-infected cells by IFA. JAR cell clone #4 lacking *SGMS1* were transiently express the indicated genes fused to mApple, followed by infection of either RV$_{VAC}$ (upper panels) or RV$_{FI}$ (lower panels) at 2 days post transfection. RV antigens were detected by IFA at 4 days post transfection, as shown in green. Parental JAR cells were shown as a positive control. A red fluorescent protein mCherry was used as a vector control. Blue represents the DAPI-stained nucleus; magnification 400×. Scale bar, 10 μm.

(C and D) Effect of the stable expression of indicated genes in either *SGMS1*-null JAR cell clone #4 (C) or parental JAR cells (D) on RV$_{VAC}$ infection. Each gene was fused to mApple as its carboxy terminus. RNA was recovered from the tissue culture medium at 9 days post infection and subjected to the real-time PCR. For the control, G418 resistance gene was transduced (C). The average values and the standard deviation (SD) of three independent wells are shown. Gray indicates the range of the control levels (Figure 2E), and the dashed line indicates the limit of detection (5 copies/reaction). Asterisk, p < 0.001 compared to the control shown in Figure 2E, examined in parallel.

(E) Sphingomyelin content in *SGMS1*-null JAR cell clone #4, stably expressing the indicated genes fused to mApple. The concentrations corresponding to 1×10^6 cells lysed in 50 μL assay buffer are shown. The dashed line represents the parental cell levels (Ctr in Figure 2D).

Property of SGMS1 that supported RV infection

SGMS1 is part of a gene family that includes *SGMS2* and *SMSr*, all of which possess ceramide phosphoethanolamine synthetase activity. However, only SGMS1 and SGMS2 exhibit SGM synthase activity. SGMS1 provides the major SGM synthase activity in mammalian cells.[20] SGMS2 and SMSr share amino acid homologies of 61.7% and 37.2%, respectively, when compared to SGMS1. These genes are ubiquitously expressed in tissue culture cell lines, as determined by our study and previous reports (Document S1). Our study detected abundant levels of SGMS1 and SMSr in human cell lines of various origins, regardless of their susceptibility to RV, as assessed by RT-PCR. *SGMS2* was faintly detectable in some cell lines, and its detection could have been challenging since it has several splice variants. To verify the SGM synthase activity in SGMS1-, SGMS2-, and SMSr-mApple, we expressed each of them constitutively in *SGMS1*-null cells. SGM synthase activity was confirmed in SGMS1- and SGMS2-mApple, but not in SMSr-mApple (Figure 3E). Interestingly, ectopic expression of SGMS2-mApple, but not SMSr-mApple, rendered cells susceptible to RV infection, albeit slightly less efficiently than SGMS1-mApple (Figures 3B and 3C). We did not initially detect *SGMS2* in our genetic screen, likely due to its lower expression levels in JAR cells compared to *SGMS1*. To investigate the contribution of SGM synthase activity to RV infection, we constructed an SGMS1 mutant bearing a D332A mutation, which affects the HHD motif at the 3rd extracellular loop and 4th and 6th membrane-spanning domains (Figure 2A). Stable expression of SGMS1^{D332A}-mApple increased the SGM content in *SGMS1*-null JAR cell clone #4 to levels similar to those of SGMS1-mApple, indicating that SGM synthase activity was intact in the mutant (Figure 3E). However, SGMS1^{D332A}-mApple failed to restore the cellular susceptibility to RV infection (Figures 3B and 3C). These data suggest that the physical presence of SGMS1 protein may be crucial for cellular susceptibility to RV infection in JAR cells.

Restricted process in the early phase of RV's life cycle

Initial experiments indicated that RV replication is limited in JAR *SGMS1*$^{-/-}$ cell clones, likely due to a restriction in the early stages of viral life cycle (Figure 2E). To further investigate this restriction, we examined the attachment of RV to the cell surface. Cells were exposed to viruses either RV$_{FI}$ or RV$_{VAC}$ at 4°C for 30 min, and the amount of cell-associated virus was then measured using real-time RT-PCR after washing intensively with PBS. We found that the amount of cell-associated virus on *SGMS1*-null cell clone #4 was comparable to that

Table 1. Efficiency of RV attachment onto JAR cells expressing SGMS1

Virus	Experiments	Cells[a]	RV viral RNA[b]	% control
RV$_{VAC}$	1	SGMS1-null	2.5 ± 0.1	136.0
		SGMS1-mApple	3.4 ± 0.1	
	2	SGMS1-null	2.1 ± 0.1	98.9
		SGMS1-mApple	2.1 ± 0.1	
	3	SGMS1-null	5.1 ± 0.2	101.7
		SGMS1-mApple	5.2 ± 0.6	
RV$_{FI}$	1	SGMS1-null	1.3 ± 0.1	60.4
		SGMS1-mApple	0.8 ± 0.1	
	2	SGMS1-null	1.2 ± 0.1	197.0
		SGMS1-mApple	2.4 ± 0.1	
	3	SGMS1-null	7.4 ± 0.2	105.4
		SGMS1-mApple	7.8 ± 0.6	

[a]Tested cells were derived from JAR SGMS1-null cell clone #4 either constitutively expressing mCherry (SGMS1-null) or SGMS1-mApple.
[b]RV viral genome copy number assessed by quantitative RT-PCR (× 10³ copies/reaction) The average value and the standard deviation of three independent reactions are shown.

on the cells expressing SGMS1-mApple (116.6 ± 46.2%, average and SD of six independent experiments, Table 1), suggesting that viral attachment was not restricted in cells lacking SGMS1. E1 is a viral protein that binds to the surface of cells, mediating the attachment of the virus to the cells.[21] We found that the purified recombinant E1-Fc protein capable of blocking RV infection was bound to JAR cells positive for SGMS1 at similar levels to cells lacking SGMS1 as per flow cytometry results (Figure 4A). These data suggested that viral attachment was not restricted in the JAR cells lacking *SGMS1*. Previous studies have shown that SGMS1 regulates transferrin-induced clathrin-dependent endocytosis,[22,23] while RV enters cells via clathrin-dependent endocytosis.[8] To determine whether *SGMS1*-deficient cells are unable to take up viruses via endocytosis, we used viral vectors as probes. Adenovirus enters cells via clathrin-dependent endocytosis.[24] VSV-G-pseudotyped MLV infects cells via endocytosis, mimicking VSV.[25–27] We found that the infection efficiencies of adenovirus and VSV-G-pseudogyped MLV were comparable between JAR cells lacking *SGMS1* and those expressing *SGMS1* (Figures 4B and 4C), indicating that *SGMS1*-null cells are competent in endocytosis. Since both adenovirus and VSV-G require endosomal acidification to establish an infection, the acidification process in the endosome must be intact in cells lacking *SGMS1*. The vacuolar proton-ATPase (V-ATPase) is the main player in endosomal and lysosomal acidification, and SGM facilitates the function of V-ATPase, enabling the maturation of early endosomes into late endosomes.[28–30] In JAR *SGMS1*$^{-/-}$ cell clones, the reduced amount of SGM might attenuate the acidification process in the endosome. To investigate this, we visualized acidic organelles using the fluorescent probe LysoPrime dye that fluoresced at pH lower than 6.0 (Figure 4D). Acidic organelles, mostly lysosomes, were detected in both SGMS1-positive and negative cells, indicating that the degradative pathway was intact regardless of *SGMS1* status. However, the fluorescent signals were fewer, fainter, and smaller in cells without SGMS1 than in cells expressing SGMS1. Parental JAR and *SGMS1*-reintroduced cells had 11.7 ± 6.4 (N = 100) and 7.3 ± 3.5 (N = 100) acidic organelle signals per cell, respectively, whereas their *SGMS1*-deficient counterparts had 1.4 ± 1.8 (N = 100) and 2.0 ± 2.8 (N = 129) per cell, respectively, examined under confocal microscopy (Figure 4D). The number of acidic organelle signals in *SGMS1*-deficient cells was significantly smaller than their SGMS1-positive counterparts (p < 0.001). These data suggested that the acidification of endosomes does not proceed effectively in cells lacking *SGMS1*.

Restriction in the late phase of RV's life cycle

To test if JAR *SGMS1*$^{-/-}$ cells could support persistent infection of RV, we transfected *SGMS1*-null JAR cell clone #4 with a plasmid co-expressing SGMS1-mApple and mouse CD4. Cells were selected using magnetic beads directed toward mouse CD4, and exposed to RV$_{VAC}$. The cells were then subjected to the limiting dilution cloning in a 96-well plate, and the emerged cells were examined for RV antigen expression by IFA. Out of the 30 wells that cells emerged in, one well was positive for RV antigens (3.3%, Table 2). However, the percentage of RV antigen-positive cells was approximately 10%. These cells were subjected to another round of limiting dilution cloning. Out of the 40 wells in which cells emerged, two were positive for cells with RV antigens (5.0%). However, the percentage of RV antigen-positive cells was 10% and 40%, respectively (Table 2). To confirm the clonality of these cells, one of the cells was subjected to the limiting dilution cloning. Among 41 wells positive for the cell outgrowth, 14 were positive for the cells bearing RV antigens (34.1%). However, similar to the previously described experiments, the percentage of RV antigen-positive cells was at most 70%. In the control experiment, the parental JAR cells persistently infected with RV were tested. Almost all the cells that emerged in the 96-well plate (35/36 wells, 97.2%) were RV antigen positive, and the percentage of RV antigen-positive cells was higher than 90% (Table 1).

We further analyzed three RV antigen-positive cell clones #4-L4, L9, and L22, which emerged in the third limiting dilution cloning experiment (denoted by superscript c in Table 2). The percentage of RV antigen-positive cells was approximately 40%, 60%, and 70%, for #4-L4, L9,
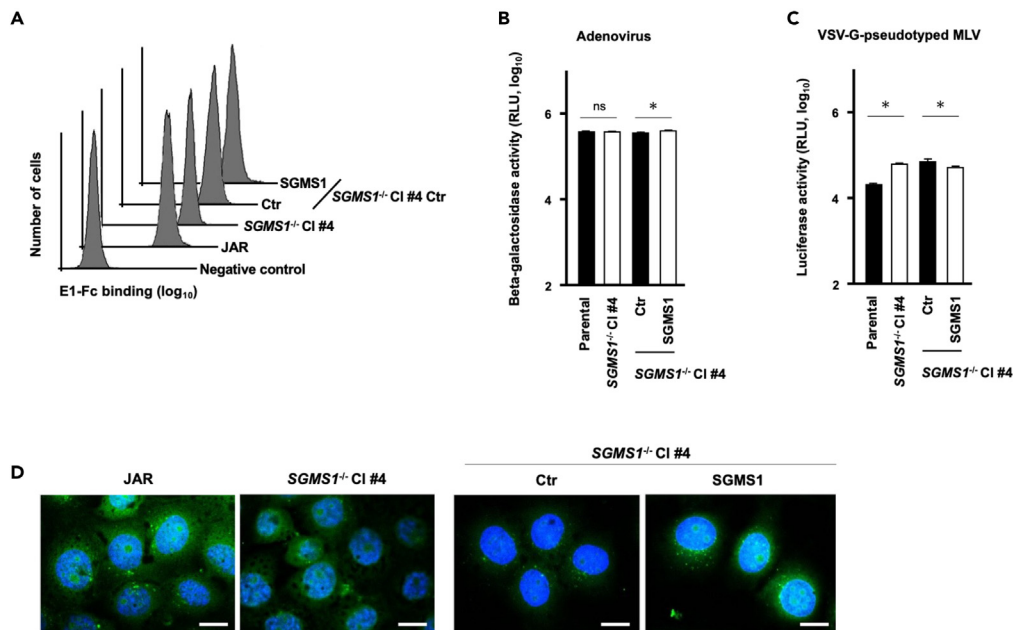
Figure 4. Effect of loss of *SGMS1* expression on the early phase of viral replication cycle

(A) Binding of recombinant purified E1-Fc on JAR cells was examined by flow cytometry. Cells were treated with 5 ng/mL E1-Fc, followed by anti-human goat IgG and anti-goat rabbit IgG conjugated with Alexa 488. X axis represents the green fluorescence reflecting the E1-Fc binding. Negative control represents JAR cells without anti-human goat IgG. Ctr, control cells transduced with mCherry gene.

(B and C) Susceptibility of JAR cells with or without SGMS1 to adenovirus (B) and VSV-pseudotyped MLV (C) vectors. The adenovirus and MLV vectors encoded beta-galactosidase and firefly luciferase expression cassettes, respectively. The average values and the standard deviation (SD) of three independent wells are shown. Ctr, control cells transduced with mCherry gene; RLU, relative light unit; ns, not significant.

(D) Detection of acidic compartments by confocal microscopy in the cells analyzed in (B) and (C), respectively. Green represents the acidic organelles bearing pH lower than 6.0 and blue represents the DAPI-stained nucleus. Magnification, 400×. Scale bar, 10 μm.

and L22, respectively. The cells were confirmed negative for *SGMS1*-mApple as assessed by RT-PCR (data not shown). Viral antigens visualized in IFA were accumulated in the cell cytoplasm, yielding punctate signals (Figure 5A). However, the fluorescence intensity and the number of the puncta were lower in *SGMS1*$^{-/-}$ cell clones than in the parental JAR cells persistently infected with RV. Soon after the limiting dilution cloning, the copy numbers of viral genomic RNA in the *SGMS1*$^{-/-}$ cell clones were comparable to the parental levels. However, they were decreased upon the cell passage in JAR *SGMS1*$^{-/-}$ cell clones, whereas no such effect was observed in the parental JAR cells (Figure 5B). The magnitude of reduction of viral genomic RNA was on average 601.2-fold after 61 days of culture. The copy numbers of viral genomic RNA in the culture supernatant were parallel to those in cell-derived RNA (Figure 5B). The RV antigen positivity was decreased by 29.8% on average of the three cell clones as assessed by IFA after 141 days (Figure 5B). The estimated appearance rate of virus-uninfected cells was 0.136 per cell generation. Reduction of viral capsid antigen expression was also observed in western blot analysis (Figure 5C). These data suggest that the late phase of the viral life cycle was restricted in JAR *SGMS1*$^{-/-}$ cells. The replication step likely affected the most was transcription and/or translation in the late phase of the viral life cycle. The instability of viral persistence was partly attributable to inefficient viral RNA amplification.

DISCUSSION

We provide evidence that *SGMS1* plays a role in supporting RV infection at both the early and the late phases of the viral life cycle. This is the first documentation of a dual-acting positive regulatory factor for RV replication.

SGMS1 is an enzyme that transfers the phosphocholine head group of phosphatidylcholine onto ceramide to produce ceramide phosphocholine, alternatively called SGM, with diacylglycerol as a byproduct. The effect of SGM content or metabolism on viral replication has been reported for some viruses. Specifically, genetic loss of *SGMS1* has been reported to lead to cell resistance to the human influenza virus (hIFV), Japanese encephalitis virus (JEV), and pseudorabies virus (PrV). More recently, *SGMS1* was identified as a positive regulator of RV infection.[31] Early stages of viral infection were found to be affected in JEV, PrV, and RV.[31-33] In the case of JEV, virus attachment of the virus was strongly affected in *SGMS1/SGMS2* double-knockout cells. Interestingly, the re-introduction of SGMS1, but not SGMS2, restored the cellular susceptibility to JEV infection, suggesting that SGMS1 and SGMS2 function differently.[32] hIFV infects cells via endocytosis and requires low pH for membrane fusion to occur.[34] However, rather than the entry, post-translational processes were attenuated for hIFV.[17] In our study, the

Table 2. Assessment of viral persistence in JAR cells lacking SGMS1 by limiting dilution cell cloning

Experiment	Initial cell status		After limiting dilution				# of wells with cells bearing given viral antigen positivity (%)									
	Viral antigen-positive cells (%)	# of 96-well plates	# of wells positive for cells	% of wells with cell emergence[a]	# of wells positive for cells expressing viral antigens	% of wells with viral antigen-positive cell	0~	10~	20~	30~	40~	50~	60~	70~	80~	90~
1	NA	5	30	6.3%	1	3.3%	29	1[b]	0	0	0	0	0	0	0	0
2	~10	5	40	8.3%	2	5.0%	38	1	0	0	1[c]	0	0	0	0	0
3	~40	10	41	4.3%	14	34.1%	27	3	5	3	1[d]	0	1[d]	1[d]	0	0
Control	~100	5	36	7.5%	35	97.2%	1	0	0	0	0	0	0	0	0	35

NA, not assessed.

[a]Number of wells emerged with cell colonies per number of wells into which cells were seeded.

[b]Subjected to the limiting dilution cloning in the next round.

[c]Subjected to the limiting dilution cloning in the next round.

[d]Subjected to further analysis (see text).
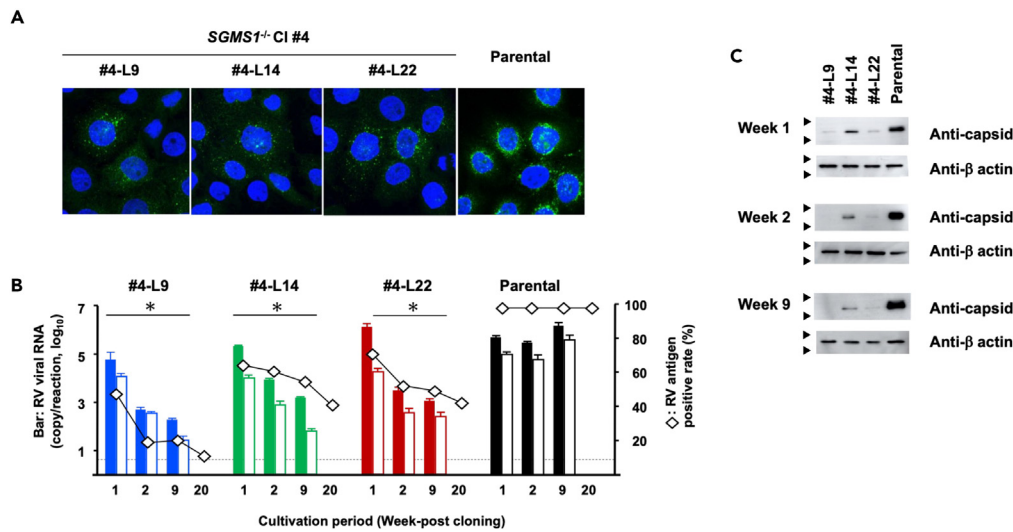
Figure 5. Effect of loss of *SGMS1* expression on the late phase of viral replication cycle

(A) Detection of RV antigens by IFA. JAR cell clone #4 lacking *SGMS1* was infected with RV$_{VAC}$ and subjected to the limiting dilution. Three clones were tested for viral antigen, as shown in green. A parental JAR cells infected with rubella virus were used as a control (Parental). Blue represents the DAPI-stained nucleus; magnification 400×. Scale bar, 10 μm.

(B) Loss of rubella viral RNA and protein from JAR cell clone lacking *SGMS1*. Three cell clones isolated in the limiting dilution were maintained in cell culture and the viral RNA (left axis) and the viral antigen-positive rate was determined (right axis). The viral RNA was quantified by real-time PCR using the RNA extracted from the cells (filled) or from the culture medium (open) at the indicated weeks after clones were established. Shown are the average and the standard deviation (SD) of three independent reactions. RV antigen-positive rate was examined by IFA; it is indicated by the diamond symbols. The dashed line indicates the limit of detection (5 copies/reaction). Asterisk represents *p* value less than 0.05 compared to the corresponding parental data by Student's *t* test, two-sided.

(C) Immunoblotting for RV capsid antigen or beta actin (loading control) detection in JAR cell clone lacking *SGMS1* infected with RV. The triangles of the anti-capsid blots represent 37 and 25 kDa of the molecular weight markers, respectively. The triangles of the anti-β actin blots represent 50 and 37 kDa of the molecular weight markers, respectively.

attachment of RV onto the cells was found to be unaffected by *SGMS1* deficiency, and both *SGMS1* and *SGMS2* supported RV infection. Our results suggest that *SGMS1* does not serve as an RV receptor, and highlighting the unique nature of RV.

Membrane microdomains are portions of the plasma membrane that are rich in SGM and cholesterol; they serve as a platform to receive cytokines and chemokines, initiate signal transduction, trigger endocytosis, and act as a portal for some viruses to infect cells.[35] Otsuki N. et al. has reported that SGM plays a role in the binding of RV virions to the cell surface via viral E1 envelope glycoprotein.[36] Our data suggested that the RV life cycle is restricted in *SGMS1*-null JAR cells, particularly during the steps following adsorption and at or before the initiation of viral gene transcription. We considered the possibility that acidification-dependent processes are targeted by SGMS1. Membrane fusion between the RV envelope and endosomal membrane is mediated by the viral glycoprotein E1. Acidic conditions trigger conformational changes in E1, which initiate membrane fusion. Additionally, capsid uncoating of RV also requires a low pH. The acidic environment in the endosome induces conformational changes in the viral capsid protein, allowing the uncoating of RV. The two processes require a distinct degree of acidification. While the former is induced the most efficiently at pH 6.0–6.2,[9,37] the latter is induced at pH 5.0–5.5.[38] Adenovirus enters cells via endocytosis and requires an acidic environment pH 6.0 to penetrate the early endosomal membrane and establish infection.[24,39] VSV infects cells via endocytosis, requiring exposure to an acidic environment at pH 6.5 in the early endosome,[27] thereby suggesting that VSV-G-pseudotyped MLV behaves similarly to VSV.[40] Given that adenovirus and VSV-G-pseudotyped MLV infect JAR *SGMS1*$^{-/-}$ cells efficiently, the acidification should proceed to ensure pH 6.0 in the endosome, which would then cause RV E1 to undergo a conformational change. Further acidification of the virus-containing endosomes may be attenuated, preventing the priming of the RV uncoating process. Unless the appropriate acidification occurs in a timely manner, the virus-containing endosomes would fuse with lysosomes, and the virus would be degraded. Recently, Mori et al. suggested that RV infection was restricted in JAR *SGMS1*$^{-/-}$ cells at the membrane fusion step.[31] Our findings were consistent with their findings since insufficient acidification of endosomes should result in the block of Env conformational change to endorse virus-cell membrane fusion. Even if membrane fusion occurred, transcription of viral RNA would not be initiated without the priming of the capsid uncoating. Disturbance of endosomal acidification is likely due to the attenuated V-ATPase function without the sufficient levels of SGM.[28–30] A mutant of *SGMS1* bearing SGM synthase activity failed to restore the susceptibility of JAR *SGMS1*$^{-/-}$ cells to RV infection in the transient transfection experiment. These data probably suggested that the enzyme activity of the mutant SGMS1 was not high enough to support RV infection in the transient experimental settings whereas the accumulation of SGM could be restored in the long-term cultivation. Another possibility to address is the amount of ceramide that should be increased in *SGMS1*$^{-/-}$ cells.[19,41–43] We have not investigated the endosomal calcium concentrations in our study since no reports have suggested a direct link between SGMS1 and calcium metabolism in the endosome. However, this is an open possibility to address in the future.

Our data suggest that *SGMS1* plays a role in the late phase of RV's life cycle. We demonstrated RV persistency in human placenta-derived cell lines, which contrasted with previous findings by Adamo et al., in which RV infection induced apoptosis in primary cells derived from the human placenta.[44] In the persistently infected JAR *SGMS1*$^{-/-}$ cells, the viral genomic RNA and the viral protein levels were both reduced. Thus, the affected step was at or before the transcription/translation of the viral genes, despite the two steps being coupled to each other. The Golgi apparatus consists of RV's RC.[10,11] SGMS1 is mostly localized to the Golgi apparatus.[20] The structure and function of the Golgi apparatus depend on *de novo* synthesized SGM.[45] The deficiency of *SGMS1* may affect RV replication through the dysfunction of the Golgi complex. Consistent with our observation, viral transcription was downregulated, albeit modestly, in the transient reporter assay shown by Mori et al.[31] They suggested that the late phase of RV life cycle was unaffected in JAR *SGMS1*$^{-/-}$ cells. In our study, the RV persistence was monitored for more than 20 weeks after infection of JAR *SGMS1*$^{-/-}$ cells with RV. The previous study did not assess the long-term maintenance of RV replicon, which explained the difference between the two. This study provides the first genetic evidence that identifies a host factor affecting the persistence of RV infection. Multiple RC foci were present in the cytoplasm, distributed around the nucleus, as visualized by IFA. The appearance of RV antigen-negative cells from virus-infected cells suggests that SGMS1 contributes to either the maintenance of the RC or the distribution of RC onto the daughter cells, or both. When the number of replication foci became few, a daughter cell might fail to inherit the viral replication machinery. The segregation process of the RV's RC, once the mechanisms are clarified, can be targeted to interfere with persistent RV infection.

Finally, our findings are relevant to the pathogenesis of mother-to-child transmission of RV and virus-induced teratogenicity. RV is detected in almost all tissues of infants infected with RV *in utero*.[2] In this study, we demonstrated that the trophoblast-derived cells are highly permissive to persistent RV infection. This suggested that the placenta can actively transmit the virus from mother to fetus. The persistence of RV in trophoblasts may interfere with the placental functions, possibly leading to the intrauterine growth restriction of the fetus. The in-depth characterization of RV-*SGMS1* interaction could contribute to the understanding of the life cycle of RV and its pathogenicity.

Limitations of the study

While genetic interactions between RV and SGMS1 have been demonstrated, it has become evident that cells lacking SGMS1 experience inhibitions during both the early and late phases of the viral life cycle. However, there is still a need to elucidate the molecular mechanisms underlying these inhibitions in each of these processes. In the early phase, the absence of SGMS1 has been suggested to interfere with endosomal acidification. However, the detailed molecular mechanism remains to be clarified. In the late phase, the precise molecular role of SGMS1 in maintaining persistent infection remains undefined. If the enzymatic function of SGMS1 plays a role in supporting viral life cycle, it is critical to determine how reductions in substrate or the accumulation of the metabolites influence RV replication. If the interaction is mediated by protein-protein interactions, a technical challenge arises due to SGMS1 being a membrane protein, which is generally difficult to handle in biochemical assays.

In this study, the cell types used for validation are limited to human placental-derived cell lines. It is unknown whether SGMS1 plays a central role in supporting RV infection in other cell types. Additionally, further investigation is needed to determine the extent of SGMS2's involvement. Lastly, addressing the role of SGMS1 in the pathogenesis of rubella and CRS requires examination within an *in vivo* context.

STAR★METHODS

Detailed methods are provided in the online version of this paper and include the following:

- KEY RESOURCES TABLE
- RESOURCE AVAILABILITY
  - ○ Lead contact
  - ○ Materials availability
  - ○ Data and code availability
- EXPERIMENTAL MODEL AND STUDY PARTICIPANT DETAILS
  - ○ Cell culture
  - ○ Plasmids
  - ○ Viruses
- METHOD DETAILS
  - ○ Genetic screen
  - ○ Quantification of sphingomyelin content
  - ○ Analysis of proteins
  - ○ Nucleic acid extraction and amplification
  - ○ Reporter assay
  - ○ Cell imaging
  - ○ Estimation of the appearance of cells without RV infection
  - ○ Statistical analysis

REFERENCES

1. Anne, A.G. (2020). Rubella Virus (German Measles). In Mandell, Douglas, and Bennett's principles and practice of infectious diseases, 9th ed., J.E. Bennett, R. Dolin, and M.J. Blaser, eds. (Elsevier Saunders), pp. 2007–2012.

2. George, S., Viswanathan, R., and Sapkal, G.N. (2019). Molecular aspects of the teratogenesis of rubella virus. Biol. Res. 52, 47.

3. Cunningham, A.L., and Fraser, J.R. (1985). rubella virus infection of human synovial cells cultured in vitro. J. Infect. Dis. 151, 638–645.

4. Williams, M.P., Brawner, T.A., Riggs, H.G., Jr., and Roehrig, J.T. (1981). Characteristics of a persistent rubella infection in a human cell line. J. Gen. Virol. 52 (Pt 2), 321–328.

5. Perelygina, L., Zheng, Q., Metcalfe, M., and Icenogle, J. (2013). Persistent infection of human fetal endothelial cells with rubella virus. PLoS One 8, e73014.

6. Rawls, W.E., Phillips, A., Melnick, J.L., and Desmond, M.M. (1967). Persistent virus infection in congenital rubella. Arch. Ophthalmol. 77, 430–433.

7. Cong, H., Jiang, Y., and Tien, P. (2011). Identification of the Myelin Oligodendrocyte Glycoprotein as a Cellular Receptor for Rubella Virus. J. Virol. 85, 11038–11047.

8. Kee, S.H., Cho, E.J., Song, J.W., Park, K.S., Baek, L.J., and Song, K.J. (2004). Effects of endocytosis inhibitory drugs on rubella virus entry into VeroE6 cells. Microbiol. Immunol. 48, 823–829.

9. Dubé, M., Rey, F.A., and Kielian, M. (2014). M. Rubella virus: first calcium-requiring viral fusion protein. PLoS Pathog. 10, e1004530.

10. Fontana, J., Tzeng, W.P., Calderita, G., Fraile-Ramos, A., Frey, T.K., and Risco, C. (2007). Novel replication complex architecture in rubella replicon-transfected cells. Cell Microbiol. 9, 875–890.

11. Magliano, D., Marshall, J.A., Bowden, D.S., Vardaxis, N., Meanger, J., and Lee, J.Y. (1998). Rubella virus replication complexes are virus-modified lysosomes. Virology 240, 57–63.

12. Sakata, M., Katoh, H., Otsuki, N., Okamoto, K., Nakatsu, Y., Lim, C.K., Saijo, M., Takeda, M., and Mori, Y. (2019). Heat Shock Protein 90 Ensures the Integrity of Rubella Virus p150 Protein and Supports Viral Replication. J. Virol. 93, e01142-19.

13. Beatch, M.D., Everitt, J.C., Law, L.J., and Hobman, T.C. (2005). Interactions between rubella virus capsid and host protein p32 are important for virus replication. J. Virol. 79, 10807–10820.

14. Ilkow, C.S., Mancinelli, V., Beatch, M.D., and Hobman, T.C. (2008). Rubella virus capsid protein interacts with poly(a)-binding protein and inhibits translation. J. Virol. 82, 4284–4294.

15. Pugachev, K.V., and Frey, T.K. (1998). Rubella virus induces apoptosis in culture cells. Virology 250, 359–370.

16. Duncan, R., Muller, J., Lee, N., Esmaili, A., and Nakhasi, H.L. (1999). Rubella virus-induced apoptosis varies among cell lines and is modulated by Bcl-XL and caspase inhibitors. Virology 255, 117–128.

17. Tafesse, F.G., Sanyal, S., Ashour, J., Guimaraes, C.P., Hermansson, M., Somerharju, P., and Ploegh, H.L. (2013). Intact sphingomyelin biosynthetic pathway is essential for intracellular transport of influenza virus glycoproteins. Proc. Natl. Acad. Sci. USA 110, 6406–6411.

18. Li, Z., Fan, Y., Liu, J., Li, Y., Huan, C., Bui, H.H., Kuo, M.S., Park, T.S., Cao, G., and Jiang, X.C. (2012). Impact of sphingomyelin synthase 1 deficiency on sphingolipid metabolism and atherosclerosis in mice. Arterioscler. Thromb. Vasc. Biol. 32, 1577–1584.

19. Tafesse, F.G., Huitema, K., Hermansson, M., van der Poel, S., van den Dikkenberg, J., Uphoff, A., Somerharju, P., and Holthuis, J.C.M. (2007). Both sphingomyelin synthases SMS1 and SMS2 are required for sphingomyelin homeostasis and growth in human HeLa cells. J. Biol. Chem. 282, 17537–17547.

20. Huitema, K., van den Dikkenberg, J., Brouwers, J.F.H.M., and Holthuis, J.C.M. (2004). Identification of a family of animal sphingomyelin synthases. EMBO J. 23, 33–44.

21. Hobman, T. (2013). Rubella virus. In Fields Virology, 6th ed., D.M. Knipe and P.M. Howley, eds. (Lippincott Williams & Wilkins), pp. 687–711.

22. Lawrence, C.M., Ray, S., Babyonyshev, M., Galluser, R., Borhani, D.W., and Harrison, S.C. (1999). Crystal Structure of the Ectodomain of Human Transferrin Receptor. Science 286, 779–782.

23. Shakor, A.B.A., Taniguchi, M., Kitatani, K., Hashimoto, M., Asano, S., Hayashi, A., Nomura, K., Bielawski, J., Bielawska, A., Watanabe, K., et al. (2011). Sphingomyelin synthase 1-generated sphingomyelin plays an important role in transferrin trafficking and cell proliferation. J. Biol. Chem. 286, 36053–36062.

24. Nestić, D., Božinović, K., Pehar, I., Wallace, R., Parker, A.L., and Majhen, D. (2021). The Revolving Door of Adenovirus Cell Entry: Not All Pathways Are Equal. Pharmaceutics 13, 1585.

25. Fan, D.P., and Sefton, B.M. (1978). The entry into host cells of Sindbis virus, vesicular stomatitis virus and Sendai virus. Cell 15, 985–992.

26. Matlin, K.S., Reggio, H., Helenius, A., and Simons, K. (1982). Pathway of vesicular stomatitis virus entry leading to infection. J. Mol. Biol. 156, 609–631.

27. Lyles, S.D., Kuzmin, I.V., and Rupprecht, C.E. (2013). Rhabdoviridae. In Fields Virology, 6th ed., D.M. Knipe and P.M. Howley, eds. (Lippincott Williams & Wilkins), pp. 885–956.

28. Chen, S.H., Bubb, M.R., Yarmola, E.G., Zuo, J., Jiang, J., Lee, B.S., Lu, M., Gluck, S.L., Hurst, I.R., and Holliday, L.S. (2004). Vacuolar H+-ATPase binding to microfilaments: regulation in response to

phosphatidylinositol 3-kinase activity and detailed characterization of the actin-binding site in subunit B. J. Biol. Chem. *279*, 7988–7998.

29. Mindell, J.A. (2012). Lysosomal acidification mechanisms. Annu. Rev. Physiol. *74*, 69–86.

30. Lafourcade, C., Sobo, K., Kieffer-Jaquinod, S., Garin, J., and van der Goot, F.G. (2008). Regulation of the V-ATPase along the endocytic pathway occurs through reversible subunit association and membrane localization. PLoS One *3*, e2758.

31. Mori, Y., Sakata, M., Sakai, S., Okamoto, T., Nakatsu, Y., Taguwa, S., Otsuki, N., Maeda, Y., Hanada, K., Matsuura, Y., and Takeda, M. (2022). Membrane Sphingomyelin in Host Cells Is Essential for Nucleocapsid Penetration into the Cytoplasm after Hemifusion during Rubella Virus Entry. mBio *13*, e0169822.

32. Taniguchi, M., Tasaki, T., Ninomiya, H., Ueda, Y., Kuremoto, K.I., Mitsutake, S., Igarashi, Y., Okazaki, T., and Takegami, T. (2016). Sphingomyelin generated by sphingomyelin synthase 1 is involved in attachment and infection with Japanese encephalitis virus. Sci. Rep. *6*, 37829.

33. Hölper, J.E., Grey, F., Baillie, J.K., Regan, T., Parkinson, N.J., Höper, D., Thamamongood, T., Schwemmle, M., Pannhorst, K., Wendt, L., et al. (2021). A Genome-Wide CRISPR/Cas9 Screen Reveals the Requirement of Host Sphingomyelin Synthase 1 for Infection with Pseudorabies Virus Mutant gD(-)Pass. Viruses *13*, 1574.

34. Shaw, M.L., and Palese, P. (2013). Orthomyxoviridae. In Fields Virology, 6th ed., D.M. Knipe and P.M. Howley, eds. (Lippincott Williams & Wilkins), pp. 1151–1185.

35. Laude, A.J., and Prior, I.A. (2004). Plasma membrane microdomains: organization, function and trafficking. Mol. Membr. Biol. *21*, 193–205.

36. Otsuki, N., Sakata, M., Saito, K., Okamoto, K., Mori, Y., Hanada, K., and Takeda, M. (2018). Both Sphingomyelin and Cholesterol in the Host Cell Membrane Are Essential for Rubella Virus Entry. J. Virol. *92*, e01130-17.

37. Katow, S., and Sugiura, A. (1988). A Low pH-induced Conformaional Change of Rubella Virus Envelope Proteins. J. Gen. Virol. *69*, 2797–2807.

38. Mauracher, C.A., Gillam, S., Shukin, R., and Tingle, A.J. (1991). pH-Dependent Solubility Shift of Rubella Virus Capsid Protein. Virology *181*, 773–777.

39. Wiethoff, C.M., Wodrich, H., Gerace, L., and Nemerow, G.R. (2005). Adenovirus protein VI mediates membrane disruption following capsid disassembly. J. Virol. *79*, 1992–2000.

40. Johannsdottir, H.K., Mancini, R., Kartenbeck, J., Amato, L., and Helenius, A. (2009). Host cell factors and functions involved in vesicular stomatitis virus entry. J. Virol. *83*, 440–453.

41. Villani, M., Subathra, M., Im, Y.B., Choi, Y., Signorelli, P., Del Poeta, M., and Luberto, C. (2008). Sphingomyelin synthases regulate production of diacylglycerol at the Golgi. Biochem. J. *414*, 31–41.

42. Separovic, D., Semaan, L., Tarca, A.L., Awad, Maitah, M.Y., Hanada, K., Bielawski, J., Villani, M., and Luberto, C. (2008). Suppression of sphin,gomyelin synthase 1 by small interference RNA is associated with enhanced ceramide production and apoptosis after photodamage. Exp. Cell Res. *314*, 1860–1868.

43. Li, Z., Hailemariam, T.K., Zhou, H., Li, Y., Duckworth, D.C., Peake, D.A., Zhang, Y., Kuo, M.S., Cao, G., and Jiang, X.C. (2007). Inhibition of sphingomyelin synthase (SMS) affects intracellular sphingomyelin accumulation and plasma membrane lipid organization. Biochim. Biophys. Acta *1771*, 1186–1194.

44. Adamo, P., Asís, L., Silveyra, P., Cuffini, C., Pedranti, M., and Zapata, M. (2004). M. Rubella virus does not induce apoptosis in primary human embryo fibroblast cultures: a possible way of viral persistence in congenital infection. Viral Immunol. *17*, 87–100.

45. Campelo, F., van Galen, J., Turacchio, G., Parashuraman, S., Kozlov, M.M., García-Parajo, M.F., and Malhotra, V. (2017). Sphingomyelin metabolism controls the shape and function of the Golgi cisternae. Elife *6*, e24603.

46. Komano, J., Miyauchi, K., Matsuda, Z., and Yamamoto, N. (2004). Inhibiting the Arp2/3 complex limits infection of both intracellular mature vaccinia virus and primate lentiviruses. Mol. Biol. Cell *15*, 5197–5207.

47. Shishido, A., and Ohtawara, M. (1976). Development of attenuated rubella virus vaccines in Japan. Jpn. J. Med. Sci. Biol. *29*, 227–253.

48. Earley, E., and Johnson, K. (1988). The Lineage of vero,vero 76 and Its Clone C1008 in the United States. In VERO cells: origin, properties and biomedical applications, B. Simizu and T. Terasima, eds. (Department of Microbiology School of Medicine Chiba University), pp. 26–29.

49. Kanbayashi, D., Kurata, T., Takahashi, K., Kase, T., and Komano, J. (2018). A novel cell-based high throughput assay to determine neutralizing antibody titers against circulating strains of rubella virus. J. Virol. Methods *252*, 86–93.

50. Takeda, S., Kanbayashi, D., Kurata, T., Yoshiyama, H., and Komano, J. (2014). Enhanced susceptibility of B lymphoma cells to measles virus by Epstein-Barr virus type III latency that upregulates CD150/signaling lymphocytic activation molecule. Cancer Sci. *105*, 211–218.

51. Koike-Yusa, H., Li, Y., Tan, E.P., Velasco-Herrera, M.D.C., and Yusa, K. (2014). Genome-wide recessive genetic screening in mammalian cells with a lentiviral CRISPR-guide RNA library. Nat. Biotechnol. *32*, 267–273.

52. Tzelepis, K., Koike-Yusa, H., De Braekeleer, E., Li, M., Metzakopian, E., Dovey, O.M., Mupo, A., Grinkevich, V., Li, Y., Mazan, M., et al. (2016). A CRISPR Dropout Screen Identifies Genetic Vulnerabilities and Therapeutic Targets in Acute Myeloid Leukemia. Cell Rep. *17*, 1193–1205.

53. Okamoto, K., Mori, Y., Komagome, R., Nagano, H., Miyoshi, M., Okano, M., Aoki, Y., Ogura, A., Hotta, C., Ogawa, T., et al. (2016). Evaluation of sensitivity of TaqMan RT-PCR for rubella virus detection in clinical specimens. J. Clin. Virol. *80*, 98–101.

54. Hummel, K.B., Lowe, L., Bellini, W.J., and Rota, P.A. (2006). Development of quantitative gene-specific real-time RT-PCR assays for the detection of measles virus in clinical specimens. J. Virol. Methods *132*, 166–173.

55. Kurata, T., Kanbayashi, D., Komano, J., and Motomura, K. (2021). Relationship between biochemical markers and measles viral load in patients with immunologically naive cases and secondary vaccine failure: LDH is one of the potential auxiliary indicators for secondary vaccine failure. Microbiol. Immunol. *65*, 265–272.

STAR★METHODS

KEY RESOURCES TABLE

REAGENT or RESOURCE	SOURCE	IDENTIFIER
Bacterial and virus strains		
Rubella virus vaccine strain	BIKEN, Osaka, Japan	N/A
Rubella virus circulating isolate	Osaka Institute of Public Health	N/A
Experimental models: Cell lines		
JAR cells	American Type Culture Collection	HTB-144
JEG3 cells	American Type Culture Collection	HTB-36
Deposited data		
Confocal micrographic images	Mendeley Data	https://doi.org/10.17632/6c64ppnx8f.1
Western blot images	Mendeley Data	https://doi.org/10.17632/6c64ppnx8f.1
Agarose gel electrophoresis image	Mendeley Data	https://doi.org/10.17632/6c64ppnx8f.1
Flow cytometric data	Mendeley Data	https://doi.org/10.17632/6c64ppnx8f.1
Recombinant DNA		
Gene knock-out vectors and mammalian expression vectors related to SGMS1, SGMS2 and SMSr	VectorBuilder	VB200803-1147nch; VB160923-1033trt; VB190602-1071dgq; VB200730-1155jxw; VB200928-1282cbg; VB210117-1177vqg; VB210824-1257hkm; VB200804-1173dpk; VB220224-1113cur; and VB210118-1185hjb

RESOURCE AVAILABILITY

Lead contact

Further information and requests for resources and reagents should be directed to and will be fulfilled by the lead contact, Jun Komano (jun.komano@ompu.ac.jp).

Materials availability

Cell lines JAR and JEG3 used in this study are available from American Type Culture Collection. Other cell lines are commercially available or provided by the lead contact upon request. The vaccine strains of rubella and measles virus are commercially available. The circulating isolate of rubella virus is provided by the lead contact upon request. Plasmids generated in this study are available from a commercial resource. Any additional materials reported in this paper is available from the lead contact upon request.

Data and code availability

Original Western blot and confocal micrography images have been deposited at Mendeley and are publicly available as of the date of publication. The genetic screen result is summarized in an excel file and deposited at Mendeley. The DOI is listed in the key resources table. Any additional information required to reanalyze the data reported in this paper is available from the lead contact upon request.

EXPERIMENTAL MODEL AND STUDY PARTICIPANT DETAILS

Cell culture

JAR and JEG3 cells were obtained from American Type Culture Collection (HTB-144 and HTB-36, respectively). 293FT cells were purchased from Invitrogen (Tokyo, Japan). Cells were maintained in RPMI-1640 medium (Nacalai Tesque, Kyoto, Japan) supplemented with 10% FBS (Lot no. 173012, Sigma-Aldrich, Tokyo, Japan), 100 U/mL penicillin, and 100 mg/mL streptomycin (Fujifilm Wako Pure Chemical, Osaka, Japan), at 37°C in a humidified 5% CO_2 atmosphere. Hygromycin (Fujifilm), G418 (Fujifilm), and puromycin (Sigma) were used at concentrations of 500, 500, and 1 μg/mL, respectively. Cells were transfected using either Lipofectamine 2000 (Invitrogen) or polyethylenimine. Magnetic cell

separation was performed using anti-mouse CD4-conjugated magnetic beads (BD Biosciences, San Jose, CA). Limiting dilution cell cloning was performed by seeding cells at 0.3 cells per well in 96-well plates.

Plasmids

The plasmid vectors used to in this study were purchased from VectorBuilder (Kanagawa, Japan). The vector IDs, which can be used for retrieving detailed information on the vector on vectorbuilder.com, are as follows: *SGMS1* knockout vector, VB200803-1147nch; mammalian expression vectors for SpCas9, VB160923-1033trt; mCherry, VB190602-1071dgq; SGMS1-mApple, VB200730-1155jxw; SGMS2-mApple, VB200928-1282cbg; SMSr-mApple, VB210117-1177vqg; fSGMS1-mApple, VB210824-1257hkm; dSGMS1-mApple carrying D332A, VB200804-1173dpk; SGMS1-mApple and mouse CD4 under the bicistronic expression system using Thosea asigna virus 2A (T2A), VB220224-1113cur; and a bacterial expression vector for E1-Fc, VB210118-1185hjb. Plasmids expressing SpCas9 and mApple fusion proteins encoded hygromycin and puromycin resistance genes, respectively. For cell cloning with G418 resistance, pcDNA3 was used (Invitrogen). Plasmid vectors required for the production of MLV vectors have been described previously.[46]

Viruses

The RV genotype 1a strain, Matsuura, was isolated from a freeze-dried live attenuated rubella vaccine (BIKEN, Osaka, Japan).[47] The endemic genotype 1E Osaka2019 RV strain was isolated from the throat swab of a patient with rubella in Osaka, Japan. Virus isolation was performed using Vero E6 cells.[48] RV was propagated in either Vero E6, RK13, or JAR cells. The tissue culture infectious dose (TCID) of RV was determined as described previously.[49] In brief, the RK13-based reporter cell line yielding luciferase upon RV infection was seeded in an 96-well plate and the virus preparation was inoculated with 10-fold serial dilutions. The luciferase positive wells were considered positive for virus infection, and the $TCID_{50}$ was calculated. For RV infection in JAR cells, $1\text{-}2 \times 10^5$ cells were seeded per well in a 24-well plate a day before infection, and were exposed to 5×10^3 $TCID_{50}$ virus, corresponding to approximately 0.1 MOI in JAR cells. The MeV vaccine strain, Schwarz (Takeda Pharmaceutical, Osaka, Japan), was recovered from the vaccine formulations in B95a or Vero-SLAM cells and was propagated in BJAB-LMP1 cells.[50] The cells were exposed to MeV at 0.01 MOI in the same experimental settings. The adenovirus vector and MLV vectors have been described previously.[46]

METHOD DETAILS

Genetic screen

The knockout screening was performed according to the procedures described previously,[51,52] with the modification that the target was JAR cells. Initially, a JAR cell clone stably expressing SpCas9 was established. In brief, 3×10^8 JAR-SpCas9 cells were infected with an LV encoding a gRNA library covering all the human genes in order to produce a cell pool with approximately 30% transduction efficiency. Two days post-LV infection, cells were selected in presence of 1 μg/mL puromycin for 5 days. A total of 5×10^7 cells were exposed to RV_{FI} 0.1 multiplicity of infection (MOI) and maintained in a 15-cm tissue culture dish. At two weeks post-RV infection (5 passages after infection), the cells were harvested for genomic DNA extraction (Qiagen, Tokyo, Japan). While $2\text{-}4 \times 10^6$ cells were harvested, 1×10^7 cells were harvested for MOCK cells. DNA preparations were subjected to PCR, followed by sequencing to analyze the enrichment of LV-encoded gRNA repertoire compared to that in the RV-uninfected cells.

Quantification of sphingomyelin content

Cellular sphingomyelin content was measured using the Amplite Fluorimetric Sphingomyelin Assay Kit (AAT Bioquest, Sunnyvale, CA, USA). The fluorescence signal was detected using an Enspire plate reader (PerkinElmer Japan, Tokyo, Japan).

Analysis of proteins

Western blotting was performed as described previously,[48] using an anti-SGMS1 antibody (G-8, Santa Cruz, Dallas, TX, USA), anti-beta actin antibody (6D1, MBL, Tokyo, Japan), anti-RV capsid antibody (9B11, Abcam, Cambridge, United Kingdom), ImmPRESS Polymer Kit (Vector Laboratories, Burlingame, CA, USA), and Envision Dual Link System-HRP (Dako, Glostrup, Denmark). Chemiluminescence was generated using SuperSignal ELISA Femto reagent (Thermo Fisher Scientific, Tokyo, Japan), and the signals were detected using an Amersham Imager 600 (GE Healthcare Life Science). A mammalian expression vector for E1-Fc was transfected into 293FT cells, which were lysed in a buffer containing 150 mM NaCl, 0.5% Triton X-100, 10 mM HEPES (pH7.4), 5% glycerol, and protease inhibitor cocktail (Sigma) at 2–3 days post-transfection. The cell lysate was incubated on ice for 60 min and subsequently subjected to centrifugation. The collected supernatant was incubated overnight with microbeads conjugated with anti-FLAG monoclonal antibody M2 (Sigma) at 4°C and washed five times with a buffer containing 300 mM NaCl, 50 mM Tris-HCl (pH 7.4), 1 mM EDTA, and 1% Triton X-100. Finally, the E1-Fc was eluted in phosphate-buffered saline containing 1 mg/mL FLAG peptide (MBL) by overnight incubation at 4°C. The magnetic beads were removed by centrifugation. The purified E1-Fc was separated in SDS-PAGE gel, stained by Coomassie Brilliant Blue, and subjected to the densitometric analysis to determine the concentration using an Amersham Imager 600 in reference to bovine serum albumin.

Nucleic acid extraction and amplification

Cellular DNA was extracted using the DNeasy Blood and Tissue Kit (Qiagen). Total RNA from cells was extracted from the cells using the RNeasy Mini Kit (Qiagen). Extraction of RNA from the tissue culture medium was performed using MagLEAD 12gC (Precision System Science,

Tokyo, Japan). PCR was performed to screen *SGMS1* gene-edited cells by using primers: 5'-CAG GAA ATC AGT AGT CCC TGA AAC G-3' and 5'-GCC AAT TTA TAG TGC TTA GGC CAA C-3'. Real-time quantitative RT-PCR was performed as described previously for RV[53] and for MeV,[54,55] respectively, using the RT-PCR quick master kit (Toyobo, Osaka, Japan). The primers and the TaqMan probes used to detect RV and MeV were follows: RV, 5'-CCT AHY CCC ATG GAG AAA CTC CT C-3', 5'-AAC ATC GCG CAC TTC CCA-3', and 5' FAM-CCG TCG GCA GTT GG-MGB 3'; MeV, 5'-TGG CAT CTG AAC TCG GTA TCA C-3', 5'-TGT CCT CAG TAG TAT GCA TTG CAA-3', and 5' FAM-CCG AGG ATG CAA GGC TTG TTT CAG A-TAMRA 3'. The transcripts of *SGMS1*, *SGMS2*, *SMSr*, and *GAPDH* were detected by using the following primers: *SGMS1*, 5'-GGC TCC TGG ACA TGA TAG AAA C-3' and 5'-GTT GTG AGA GCC AGT GAT AGA C-3'; *SGMS2*, 5'-GCA AGA TGC TGT GGG ATA GT-3' and 5'-CGT AGG ATC ACT GGG TTG ATT T-3'; *SMSr*, 5'-CGA GCC TTT GCC ATT TGG AG-3' and 5'-TGG GCA GCC AAG ATG AAG AA-3'; and *GAPDH*, 5'-CCA GCT ACT CGC GGC TTT A-3' and 5'-TTC CCA TTC TCG GCC TTG AC-3'. The oligonucleotides were synthesized by Sigma.

Reporter assay

For MLV vector infection, 1-2 $\times$ 10^4 cells were seeded per well of a 96-well plate and exposed to the viral preparation the next day. The following day, the cells were replated in a fresh well. The cells were lysed and luciferase activity was measured at 3 days post-infection by using the One-Glo kit (Promega, Madison, WI), according to the manufacturer's protocol. For adenovirus vector infection, 1 $\times$ 10^4 cells were seeded per well of a 96-well plate and exposed to the viral vector the following day. The cells were lysed and the beta-galactosidase activity was measured at 2 days post-infection by using a Beta-Glo kit (Promega). Chemiluminescence was detected using an Enspire plate reader (PerkinElmer).

Cell imaging

JAR cells were plated in a well of a 24-well plate at a density of 1 $\times$ 10^5 cells per well. Cells were transfected with plasmids the next day, and re-plated in two wells of a 24-well plate. At two days post-transfection, the cells were exposed to RV at approximately 0.1 MOI. The cells were placed on a 12-well hole slide glass (TF1205, Matsunami Glass, Osaka, Japan) coated with iMatrix-511 substrate (Nippi, Tokyo, Japan) at two days post-infection, and subjected to immunofluorescence assay (IFA) at three days post-infection, as detailed below. When red fluorescence protein was visualized, the cells were placed on a glass slide at one-day post-transfection. Cells were fixed in 4% formaldehyde in PBS, stained, and mounted in Vectashield antifade mounting medium with DAPI (H-1200, Vector Laboratories, Burlingame, CA, USA). For viral antigen detection, the cells were stained with an anti-rubella virus antibody conjugated with FITC (Code 36361, GeneTex, Irvine, CA, USA). For the organelle staining, LysoPrime Green (Dojindo Laboratories, Kumamoto, Japan) was used. Cells were imaged using the confocal fluorescence microscope LCM700 (Carl Zeiss, Tokyo, Japan). The images were adjusted for brightness and contrast as visualized on the printed paper and on the screen.

Estimation of the appearance of cells without RV infection

The mammalian cell growth curve was represented by an exponential model,

$$N(X) = 2^X$$

where N(X) is the number of cells after X times of cell divisions. Considering k as the appearance rate of cells without RV infection, the number of virus-uninfected cells N$_U$(X) after X cell divisions were

$$N_U(X) = (2 - k)^X.$$

Considering that the mammalian cell division cycle takes approximately 24 h, the number of culture days equals the number of cell divisions.

Statistical analysis

Experimental results were analyzed using a two-sided Student's *t* test. Statistical significance was set at $p < 0.05$.